SEAWATER CORROSION RESISTANT HEAT TRANSFER AGENT (HTA) TO IMPROVE WATER EVAPORATION IN SOLAR STILL

(AGEN PEMINDAHAHN HABA YANG TAHAN KARAT UNTUK MENINGKATKAN PENYEJATAN AIR DALAM PENYULING SURIA)

CHEW FEW NE

SYARIFAH BINTI ABD RAHIM

CHENG CHIN KUI

RESEARCH VOTE NO.:

RDU 140368

Faculty of Chemical & Natural Resources Engineering

Universiti Malaysia Pahang

2016

ACKNOWLEDGEMENTS

First and foremost, I would like to acknowledge Universiti Malaysia Pahang through RDU140368 for funding this research project. I would also like to extend my thanks to team members who always help and gave advice and suggestion in this project. A special note of appreciation to all the staff members of FKKSA, for their professional and technical assistance. Thanks to my postgraduate and undergraduate students that work out the research plan accordingly. This project could not be fully completed without their assistances. Last but not least, to my family members. I wish to dedicate my gratitude for their continuous prayers, love and support.

ABSTRACT

SEAWATER CORROSION RESISTANT HEAT TRANSFER AGENT (HTA) TO IMPROVE WATER EVAPORATION IN SOLAR STILL

(Keywords: Solar still, heat transfer agent, corrosion, evaporation)

Solar still is an economical technique for water desalination, however its main drawback is low productivity. In this project, a heat transfer agent (HTA) was installed in a solar still aimed to distribute the heat throughout the seawater and increase the water evaporation rate. Copper was selected as the HTA due to its high electrical and thermal conductivities. However, seawater may cause copper corrosion; hence coating is required to avoid the metal deterioration. The present study reported the effects of coating material and thickness, and the incubation temperature on the copper corrosion rate and heat transfer rate. Copper rods coated with different coating material have low weight loss and corrosion rate if compared with bare copper rod. Besides, weight loss and corrosion rate with incubation temperature of 25°C were relatively high if compared with incubation temperature of 60°C. Moreover, an increase in the coating layer linearly increased the mass of the coated copper rods. Under the steady-state condition, the thermal conductivities increased when the coating layer was increased further. Hence, adding the coating layer reduced the radial heat transfer rate and higher axial heat transfer rates were obtained. A solar still was designed and fabricated. HTA consists of a sheet of copper plate and 12 pieces of copper rods. Two set of experiment set-up were conducted to investigate the effect of HTA on the solar still performance. In general, water and glass temperatures and evaporative heat transfer of solar still with HTA were higher than the solar still without HTA. Experiment data have revealed the function of the HTA that may quickly transferred the radiation energy from the copper plate and rods to the water. The introduction of the HTA has successfully increased 30% of water evaporation rate and 18% of thermal efficiency.

TABLE OF CONTENTS

LIST OF TABLES

LIST OF FIGURES

LIST OF ABBREVIATIONS

HTA	heat transfer agent
mpy	mils per year

CHAPTER 1

INTRODUCTION

1.1 Background of study, motivation and problem statement

Almost every living thing on earth depends on water and the water crisis in the world is worsening day by day. In response to the depleting amount of fresh water sources, producing water out of seawater is the most favourable alternative. In order to produce the fresh water, desalination process is required to remove dissolved salts and other unwanted impurities from the seawater. There are many methods in desalination which are broadly classified into two: thermal process and membrane process. Desalination through solar distillation is found to be the most economical technique, as it requires a free source of energy. There are many types of solar still, and the basin type solar still is reported to be the most prevalent type due to its simplicity. The main drawback of the solar still is its low productivity. Extensive research has been carried out by different organizations worldwide to develop an efficient solar still. The performance of solar stills is influenced by design, operating and environmental factors. Mechanical devices such as a solar tracker, solar collectors, condenser, and fans have become a trend for recent researches upon solar still as they seem able to improve the efficiency. This tendency has turned the solar still to be competitive to other desalination methods because the high efficiency of solar still can be obtained when the major development is applied to the systems

In order to improve the efficient of solar still, an attempt was made to increase the heat transfer rate by introducing a heat transfer agent (HTA) aimed to distribute the heat throughout the feed water. In this project, copper plate and rods was selected as the HTA. Copper is an industrial metal that have wide applications in our civilization. Copper has high electrical and thermal conductivities. It was used as conductor in electrical and electronic industry. Besides, copper are the most extensively used structural materials in industry, due to its mechanical strength, easy manufacture, formability, abundance and low cost. Copper also be used to sub merged in seawater and in seacoast. However, corrosion of copper must be addressed because copper is susceptible to oxidization in marine environment. The copper and its alloys will form thin layers of corrosion products, generally brown-greenish or green-bluish, called

patina which protects the metal against subsequent deterioration in polluted atmosphere of chlorides.

Corrosion can lead to loss of mechanical strength and also structural failure. Rates of corrosion can be affected by many factors such as diffusion, temperature, conductivity, type of ions, acidity and alkalinity and electrochemical potential. The corrosion rate is heavily controlled by the diffusion of oxygen through the water to the metal surface. The industrial cost involved in preventing problems such as corrosion in every aspect is high, and so there is considerable drive from these industries to find cheap and effective additives to control these problems. In corrosive environments, mild copper structures can be protected by coating protection. Coating by using paint is a good resistance against atmospheric corrosion. However, additional layers of coating on the metal surface may increase thermal resistant and affect the heat transfer rate of the designed solar still.

1.2 Research objective

1. To design the HTA so it can transfer the highest amount of heat from the lens focus to the water to increase the water evaporation rate.
2. To synthesis the material of construction for the HTA, having high corrosion resistance and high thermal conductivity.
3. To construct the HTA from this material.

1.3 Research scope

Copper rod was chosen as the HTA for solar still design. The effects of coating material and thickness, and the incubation temperature on the copper corrosion rate and heat transfer rate were investigated. After the synthesis, HTA was constructed and installed into the solar still. Two set of experiment set-up (solar still without HTA and solar still with HTA) were conducted to investigate effect of HTA on the solar still performance.

CHAPTER 2

LITERATURE REVIEW

2.1 Copper and its alloys

Copper is one of oldest metal known to human civilization more than 10,000 years. Copper artefacts are found in many places throughout the historical record. Researchers have found that peoples in ancient Egypt were used copper alloys to make jewellery (Pappas, 2014). There are over 400 copper alloys are in use today. The application of copper and its alloys is generally classified shown as in Table 2.1 (Philip and Schweitzer, 1996).

Table 2.1: Applications of copper in daily life.

Application	Examples
Marine	Seawater supply line, shafting and marine hardware.
Fresh water	Fresh water supply line and plumbing fittings.
Industrial	Heat exchanger, condenser and chemical plant process equipment.
Electrical	Electrical wiring, connectors, printed circuit boards and semiconductor packages.
Architectural	Building fronts, downspouts, flashing, gutters, roofing and screening

2.2 Types of corrosion

2.2.1 Uniform corrosion

Uniform corrosion normally occurs on the entire surface at nearly the same rate. The metal becomes thinner thus fails to function. Usually uniform corrosion caused of the breakdown in protective coating. It is mostly happen where metal is interacting with acid, a humid atmosphere or in any solution. Uniform corrosion is easily to measure, predict and design against. Frequently, it based on size or weight of the metal. Corrosion rates for materials often expressed in mils per year. In generally, corrosion rates of less than 3 mils per year (mpy) are considered acceptable. In environments like fresh or salt water, soils, and alkaline or acid salt solutions, the rate of uniform thinning is very low. However, the corrosion rate of copper is a little faster in

oxidizing acid, sulfur-bearing compounds, NH_3 and cyanides (Philip and Schweitzer, 1996).

2.2.2 Pitting corrosion

Pitting is insidious form of corrosion. It is one of the most damaging forms of corrosion. Local corrosion resulting in holes where cavities expanding from the surface to the inside of the metal. Generally, pitting corrosion happen on passive metals and alloys such as stainless steel when the oxide film is either chemically or mechanically does not immediately re-passivate thus damaged it severely. Pitting corrosion is difficult to analyse on an experimental basis. The shape size and the depth of pitting corrosion can only be identified through metallography.

2.2.3 Galvanic corrosion

Galvanic corrosion refers to the corrosion damage induced when two dissimilar metals are coupled together in corrosive electrolyte. The anode will corroded faster which is the electronegative member of the couple while cathode will corroded slower which means cathode is the electropositive member (Dexter, 1995). Based on the position of copper in galvanic series, copper and its alloys always use as cathode. The two major factors affecting the severity of galvanic corrosion are the galvanic potential difference between the couple and the area ratio. The corrosion is severe when the galvanic potential difference is greater between the couple (Lu, 2005).

2.2.4 Crevice corrosion

Crevice corrosion usually developed a gap between two joining surfaces. It can be formed between the metal surface and another surface (metal or non-metal). It can be in the form of a hole. The damage caused by crevice corrosion is normally confined to one metal at localized area within or close to the joining surfaces. The corrosion rate of crevice is higher than on bulk. For copper and its alloys, the attack occurs on the surface outside the crevice while the crevice remains relatively corrosion-free.

2.2.5 Erosion corrosion

Erosion corrosion refers to the combined action between erosion and corrosion in the presence of a moving corrosive fluid or a metal component moving through the fluid, thus contribute to the metal loss. Copper alloys are specifically sensitive with erosion

corrosion because the corrosion rate of copper is highly accelerated when the abrasive condition is present, such as impingement of fluid streams in the pumps, valves or in pipe lines. When the fluid flows rapidly, it can strip away any protective film. If the protective surfaces are removed locally by abrasion and fresh copper alloy exposed the material deteriorates more rapidly than under the sole effects of corrosion.

2.2.6 Stress corrosion

Stress corrosion manifests itself in the form of cracks without appearance of ductility (Mars and Fontana, 2005). Residual stresses from cold working and in combination with the corrosive condition and environment which contains ammonia or moisture contribute to stress corrosion cracking in copper material. The stress corrosion cracking occur most commonly with zinc-rich brass, however pure copper can also be damaged by this type of corrosion.

2.3 Factors affecting the corrosion

2.3.1 Flow rate

Fluid velocity affects the corrosion rate of copper. The mechanical effect of flow or velocity of a fluid combined with the corrosive action of the fluid accelerated metal loss. This will lead to erosion corrosion. The initial stage involves the mechanical removal of the metal's protective film and then corrosion of bare metal by a flowing corrosive occurs. High flow rates usually happen around tube blockages, tube inlet ends or in pump impellers.

2.3.2 Temperature

Temperature may influence the corrosion rate. Previous research was done by Melchers (2001) who investigates the relationship between corrosion rate and temperature of Cu-Ni alloys in sea-water. It was reported that the highest corrosion rate was found occurred at the temperature of 18 - 28°C for long-term exposur. Copper pipes are easy to fabricate and have extensive range of fittings. Copper pipe do not rust and block up compared with galvanised steel pipe however copper pipe also have their disadvantages. Mainly, there are few mechanisms that were cause by copper corrosion. The copper used for making copper pipe is virtually pure copper

with 99.90% copper content, blue water caused by green patina on copper will never occurs if the temperature of the water is above 70°C.

2.3.3 pH

The anodic polarization of copper may result in anodic dissolution or film formation depending on the pH range. In general, when acidity increases especially at low temperature the propensity for film formation also will increases. Earlier studies on the corrosion mechanisms and products of copper corrosion were limited to either acidic or alkaline environments. Feng (1997) has investigated the copper corrosion behaviour in aqueous solutions with pH range 3 – 13 by using electrochemical and surface analysis methods. Besides, effects of pH and chloride concentration on the electrochemical corrosion of copper in aqueous sodium chloride media were studied at the micro scale using a microcapillary droplet cell and at the macro scale using a conventional large scale cell. At the micro scale, the pit initiation of copper occurs at more negative potentials for high sodium chloride concentrations and alkaline pH values. Meanwhile, at the macro scale, the pH is shown to have a greater influence on the corrosion potential (Adriaens, 2012).

2.4 Factors affecting the heat transfer agent design

2.4.1 Coating materials for corrosion protection

Corrosion control is to preserve the physical and mechanical properties of the metal during the anticipated life of the structure. There are several techniques for preventing corrosion. As an example, uniform corrosion can be prevented by using thicker materials for corrosion allowance, using paints or metallic coatings such as plating, galvanizing or anodizing. By modifying the environment and use corrosion inhibitor also can prevent uniform corrosion.

Solid particles or pigment found in paints contains solvents and thinners to control viscosity of the metal. Paints are used to beautify the looks of the material apart from that it also have ability to prevent rusting of the metal or alloy for long periods of time (Chandler, 1985). When raw material without coating is exposed to oxygen, the oxidization process will occur gradually thus create the rust. With coating of paint applied to the materials, it will seal it from air and prevent the rusting.

There are a few factors that need to consider when choosing paint such as the corrosion category of the environment and the material to be painted. According to Patrick and Gane (2007) dry coating is the best method to apply because dry coating methods approximate well to the pore structure distributions of wet applied coatings. To simplify it, the better the dispersion of the binder and pigment in the formulation mix, the better is the match with wet coating.

2.4.2 Coating materials and its thermal properties

Different types of paint material with different thermal properties affect the heat conduction. The higher the thermal conductivity, more heat energy can be conducted per square area. Table 2.2 shows thermal conductivities of different types of paint (Sudhir, 2013). For the same composition of 75% PVC, polymer EXP-C with epoxy type of polymer has the greatest thermal conductivity value if compared with EXP-A and EXP-B with acrylic type of polymer.

Table 2.2: Thermal conductivities of different types of paint.

Coating	Polymer	Polymer Type	Hollow glass microsphere (%PVC)	Silica aerogel (%PVC)	Thermal conductivity, k (W/mK)	Thermal conductivity, k (mW/mK)
Uncoated polycarbonate	N/A	N/A	N/A	N/A	0.1649	164.9
COM-1	unknown	acrylic	-	-	0.070	70
COM-2	unknown	acrylic	-	-	0.106	106
A-1	EXP-A	acrylic	75	0	0.080	80
A-2	EXP-A	acrylic	50	25	0.080	80
A-3	EXP-A	acrylic	25	50	0.130	130
A-4	EXP-A	acrylic	0	75	0.120	120
B-1	EXP-B	acrylic	75	0	0.0850	85
B-2	EXP-B	acrylic	50	25	0.0880	88
B-3	EXP-B	acrylic	25	50	0.127	127
B-4	EXP-B	acrylic	0	75	0.104	104
C-1	EXP-C	epoxy	75	0	0.107	107

2.4.3 Coating thickness

The transfer of heat by conduction is written by Fourier's law. It was found that the heat transfer rate is inversely proportional to the pathway of heat transfer. Hence, if the coating thickness is increased, the amount of heat conducted per unit area will be reduced.

2.5 Corrosion and thermal conductivity studies

Saleh and Al-Fozan (2008) have demonstrated an experiment to evaluate the effect of seawater level on corrosion behavior of different alloys which including the carbon steels, Austenitic stainless steel, copper based alloys and nickel based alloys. The specimens were exposed under different levels of seawater (above seawater level, semi-submerged and immersed fully in seawater). The experiments were carried out at room temperature with very slow seawater movement. The corrosion rate of carbon steels are the highest at three different seawater levels. Meanwhile, the nickel based alloy has the lowest corrosion rate. In marine applications, copper-nickel is widely used as valves and pump. Therefore, many researchers have investigated the behaviour of copper alloy under marine condition. Wan Nik (2011) studied the corrosion behaviour of mild steel in seawater by using weight loss method and potentiodynamic polarization test. It was reported that the corrosion rate increases with respect to immersion period.

Searle's bar describes the concept of thermal conductivity experiment. Figure 2.1 shows the schematic diagram of a conductomer (Charles, 1948). By using the conductomer, a material being heated at one end and several points across the material, the temperature is being recorded. With known amount of heat energy being supplied and known dimension of the material, the thermal conductivity of the material can be calculated.

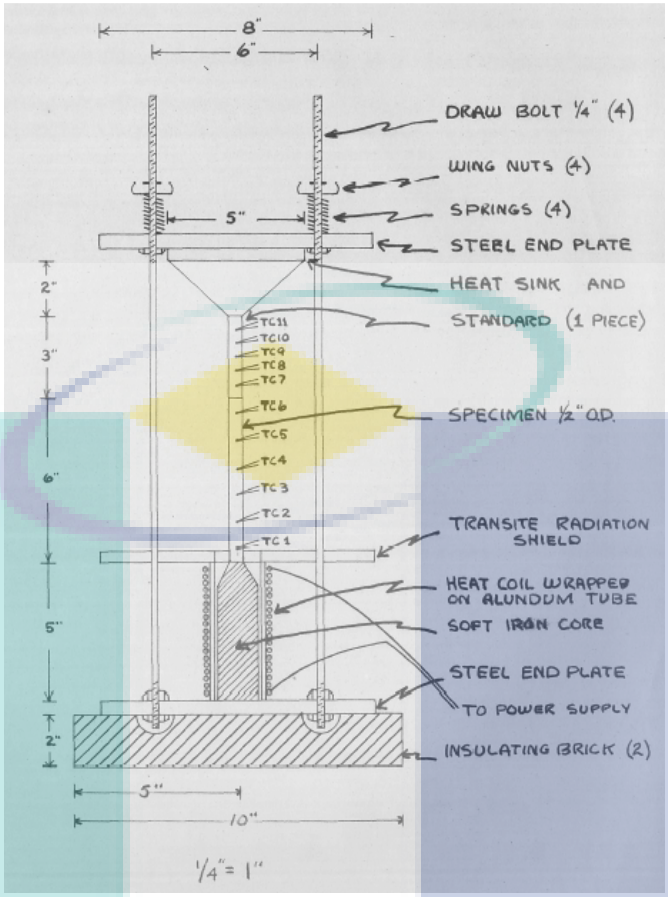

Figure 2.1: Schematic diagram of a conductomer.

2.6 Solar still

The earliest use of solar still reported dates back in 1551 by Arab chemists and then followed by several researchers including Della Porta (1589), Lavoisier (1862) and Mauchot (1869). Besides, the solar still is also reported as the oldest method of desalination used by individual or plant scale. The first successful solar still plant located at Las Salinas, Chile was built in 1872 by an engineer named Carlos Wilson from Sweden. It was the fresh water source for the mining community there for about 40 years and provides average 23 m^3 water per day (Cipollina et al., 2009).

There are numerous designs of solar still. The principle of operation is the greenhouse effect. Heat energy from the sun evaporates water inside a box covered by glass. The water condensed on the surface of the glass and dripped down into the collection container. There are so many advantages of the solar still, compared with other desalination methods, but the main problem outweighing such advantages is the low productivity. Another problem is the dependence of the solar still on an

inconsistent source of energy, such as solar radiation, has become the key of the drawback of its ability to produce freshwater compared to another method. Figure 2.2 shows a schematic diagram of a simple solar still (Bhattacharyya, 2013).

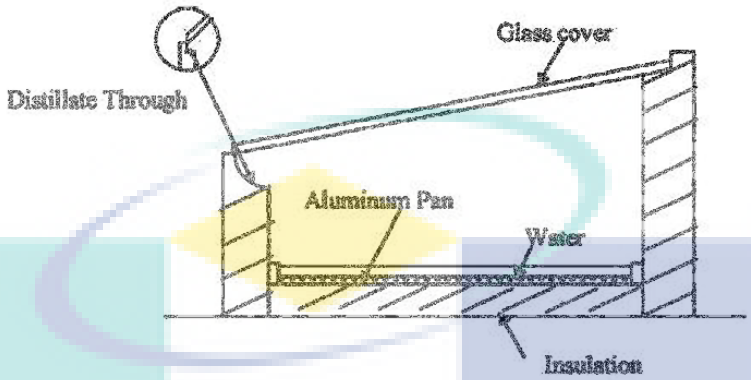

Figure 2.2: Schematic diagram of a simple solar still.

Research and development so far have yielded additional useful information on enhancing the performance of the solar still. The performance of the solar still certainly can be enhanced by improving the radiation transmission (Abdallah and Badran, 2008; Tabrizi and Sharak, 2010; Khalifa, 2011), the evaporation and/or the condensation inside the still (Rababa'h, 2003; Velmurugan et al., 2008), heat absorption (Nafey et al., 2002; Valsaraj, 2002; Kumar et al., 2008; Badran, 2007) and the level of water in the basin (Tiwari and Tiwari, 2006; Murugavel et al., 2008). The other techniques such as introducing storingmedium for the solar radiation (Abdallah et al., 2009; Tabrizi and Sharak, 2010), reusing the latent heat (Al-Karaghouli and Alnaser, 2004; Tanaka and Nakatake, 2005), separating the zone for both evaporation and condensation (Badran et al., 2004), increasing the differences of the temperature between the water surface and the cover (Zurigat and Abu-Arabi, 2004; Bechki et al., 2010), and working in sub-atomic or vacuum condition (Badran et al., 2013; Zedan and Eldin, 2015) were also reported improving the efficiency of the solar still.

2.7 Solar still with heat transfer agent

Since the beginning of the 20th century, the use of copper has been broadly extended through many demanding engineering applications; some of which are marine industry, chemical industry, automotive, solar heating, and also desalination of seawater (Davis, 2001). In the context of desalination through solar still, copper is

used either as an solar heat absorber (Eldalil, 2010; Shanmugan et al., 2012), collector (Nithin and Hraiharan, 2014) or as the main body of the still (Gnanadason et al., 2015). Gnanadason et al. (2013) study the performance of a single basin solar still made up of copper and concluded that a significant increment is achieved in productivity of the water through the solar still with the additional black paint coated inside of the basin. Earlier, it is also reported that the modified solar still basin made of copper under vacuum condition produces more evaporated water than that of copper still without vacuum (Gnanadason et al., 2011).

In another method, heating a metal surface (absorber) can be done by placing a copper plate suspended on top of the mass of the water, creating a thinly separated layer of water on one side and the rest below it as drawn in Figure 2.3 (El-Sebaii et al., 2000a). The heat absorbed by the plate from solar radiation is then transferred to heat the top surface of the water, and the remaining part of the heat is stored in the bottom water and released later during low solar intensity periods. This will ensure that continuous evaporation occurs inside the solar still regardless of it non-uniform rates (El-Sebaii et al., 2000b). Similarly, in this still, the usage of copper is tremendously elevating the water temperature due to the copper ability to conduct more heat to the water.

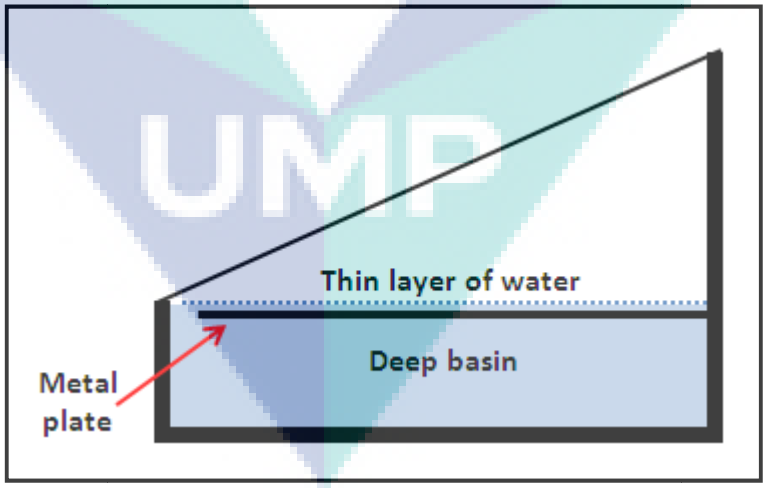

Figure 2.3: A schematic diagram of the single slope single basin solar still with baffle suspended absorber.

CHAPTER 3

MATERIALS AND METHODS

3.1 Materials for heat transfer agent analysis

In this project, the used materials for the HTA analysis are listed as below:

- Copper rods
- Spray paints (Epoxy, Ace; Polyurathane, Minwax; Enamel, Ace; Enamel, Rust-oleum)
- Seawater
- Beakers

3.2Preparation of heat transfer agent

Copper rod was chosen as the HTA for solar still design. The copper rod with same length was cut to study the effect of coating material and thickness and incubation temperature on the corrosion rate and heat transfer rate. The copper rods were cleaned to remove any possible contaminant and the mass of copper rods were measured by an analytical balance. After the mass measurement, the copper rods were spray with different paints as shown in Figure 3.1 according to the distribution in Table 3.1. The mass of copper rods with different coating material were measured again by the analytical balance.

Figure 3.1: Spray paints for copper rod coating.

Table 3.1: Types of coating materials.

Copper rod	Paint	Brand
Copper A	-	-
Copper B	Epoxy	Ace
Copper C	Polyurathane	Minwax
Copper D	Enamel	Ace
Copper E	Enamel	Rust-oleum

3.3 Effect of coating material and incubation temperature on corrosion rate

Copper rods at length of 4 cm were spray with 3 layers of coating materials as depicted in Table 3.1 and the mass of coated copper rods were determined. The copper rods were then immersed into 250 mL of seawater that prepared inside different beakers for 7 days at temperature of 25°C and 60°C. Seawater samples (10 mL) were taken in every day to determine the copper concentration in the seawater. The seawater samples were filtered through membrane filter (0.22 µm) prior the copper concentration measurement using an atomic absorption spectrometry.

After the 7 days incubation, the copper rods were taken out from the seawater and dried in an oven. The mass of each copper rod was measured again to determine the weight loss after the corrosion. Besides, corrosion rate in mils per year (mpy) was calculated from the weight loss by equation 3.1 (Kingsley and Oparaodu, 2014). CR is the corrosion rate (mil/year); W is the weight loss of the copper rod (g); ρ is the copper density (g/cm^3); A is the copper rod surface area (cm^2); T is the corrosion period (day).

$$CR = \frac{22{,}300 \times W}{\rho AT} \qquad \text{equation 3.1}$$

3.4 Effect of coating material and thickness on heat transfer rate

For studying the effect of coating material and thickness on heat transfer rate, copper rods at length of 10 cm were spray with different layers coating materials (layer 1, 2 and 3) as depicted in Table 3.1 and the mass of the coated copper rods were determined. The copper rods were then divided into three sections (Figure 3.2) and 1 cm of rod section was immersed in warm water at temperature of T_1. Heat was transfer through 7 cm of rod section ($x_2 - x_1$) and temperature at the other rod end (T_2)

was measured at steady state condition. Heat transfer process of each coated copper rod was conducted simultaneously with an uncoated copper rod, and the heat transfer rate (q) of the uncoated copper rod was determined by equation 3.2. The thermal conductivity (k) of each layer of coating materials was then calculated based on the q value.

$$q = \frac{kA}{x_2 - x_1}(T_1 - T_2)$$ equation 3.2

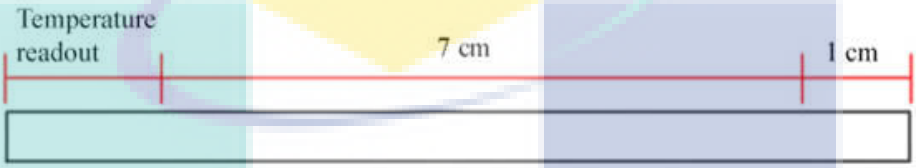

Figure 3.2: Copper rod distribution for heat transfer analysis.

3.5 Materials for solar still fabrication

In this project, the used materials for the solar still fabrication are listed as below:

- 5 pieces of 80mm x 80mm wooden boards
- 2 pieces of 50mm x 60mm wooden boards
- 2 pieces of 60mm x 60mm wooden boards
- 2 pieces of iron-free tempered glasses
- Aluminum frame
- Pipes and valves
- Silicone glue
- Copper plate with rods
- 9 pieces of magnifying glass
- Solid works software
- Aspirator pump
- Thermocouple sensor
- Pyranometer (Solar radiation meter)
- Pressure gauge

3.6 Solar still design and fabrication

Prior to the fabrication, solid works 2010 software was used to design the 3D feature solar still that based on reviewed literature and parameter studies (Singha, 2013; Bozkurt et al., 2014; Samee et al., 2007). All the fabrication process including the

metal and glass cutting, welding, drilling, sealing and painting were done by a local hardware workshop. The basin liner was fabricated as two connected basins. The external side made of wooden boards in the scale of 80 mm x 80 mm x 80 mm with 10 mm thickness whereas the internal side wooden boards in the scale of 50 mm x 60 mm x 60 mm with the same thickness. The external side of the solar still was painted in black. The further component was the top part which was made of iron free tempered glass with aluminum as the frame. The gap between the glass cover and basin liner has been sealed with silicone rubber. The basin was then connected to the outlet through a pipe and valve. Nine magnifying lenses were placed under the glass cover. An aspirator pump was also installed next to the unit together with other measurement devices including pyranometer, thermocouple sensors, and a vacuum pressure gauge. HTA consists of a sheet of copper plate and 12 pieces of copper rods that attach under the copper plate were placed inside the internal basin.

3.7 Solar still experiment analyses

Two set of experiment set-up (solar still without HTA and solar still with HTA) were conducted to investigate effect of HTA on the solar still performance. An amount of 144 L of tap water was filled into the internal wood case of solar still. Every hour from 8.00 am to 6.00 pm, the temperature readings (water, glass, ambient), solar radiation value and water level measurement were recorded. Every set of experiment were run triplicate and an average data were used for analyses. The solar still was cleaned and the wooden case was emptied after each run of experiment.

For a solar still without HTA, evaporative heat transfer between water and glass q_{ewg} was calculated by equations 3.3 to 3.8 (Garg, 2000; Al-Hussaini and Smith, 1995). q_{rga} is the radiative heat transfer from glass to the ambient air; q_{cga} is the convective heat transfer from glass to ambient air; q_{rwg} is the radiative heat transfer between water and glass; ε_g is the emissivity of the glass cover; σ is the Stefan-Boltzmann constant; T_g is the glass temperature; T_s is the radiant sky temperature; h_{ca} is the forced convection heat transfer coefficient; T_a is the ambient temperature; T_w is the water temperature.

$$q_{ewg} = q_{rga} + q_{cga} - q_{rwg} \qquad \text{equation 3.3}$$

$$q_{rga} = \varepsilon_g \sigma (T_g^4 - T_s^4) \qquad \text{equation 3.4}$$

$$q_{cga} = h_{ca}(T_g - T_a)$$ equation 3.5

$$q_{rwg} = 0.9\sigma\left(T_w^4 - T_g^4\right)$$ equation 3.6

$$T_s = T_a - 12$$ equation 3.7

$$h_{ca} = 2.8 + 3.8V$$ equation 3.8

For a solar still with HTA, evaporative heat transfer between HTA and glass q_{eHg} was calculated by equations 3.9 to 3.11 (Garg, 2000). I is the solar radiation on horizontal surface; α_H is the HTA absorptivity (based on copper); τ_g is transmissivity of the glass cover; q_{cdHw} is the conductive heat transfer between HTA and water; K is the HTA thermal conductivity; x is the HTA thickness; A_H is the HTA area and T_{HTA} is the HTA surface temperature; q_{rHg} is the radiative heat transfer between HTA and glass.

$$q_{eHg} = I\alpha_H\tau_g - q_{cdHw} - q_{rHg}$$ equation 3.9

$$q_{cdHw} = \frac{Kx}{A_H}(T_{HTA} - T_w)$$ equation 3.10

$$q_{rHg} = 0.9\sigma\left(T_{HTA}^4 - T_g^4\right)$$ equation 3.11

Thermal efficiencies of the solar still without solar still and with solar still were determined by equations 3.12 and 3.13, respectively (Garg, 2000).

$$\eta = \left(\frac{q_{ewg}}{I}\right) \times 100\%$$ equation 3.12

$$\eta = \left(\frac{q_{eHg}}{I}\right) \times 100\%$$ equation 3.13

CHAPTER 4

RESULTS AND DISCUSSION

4.1 Effect of coating material and incubation temperature on corrosion rate

In this study, bare copper rods and copper rods that coated with different coating materials (copper A to E) were immersed into seawater at temperature of 25 and 60°C for 7 days. During the 7 days incubation, the appearance of copper rods was changed. The copper rods were corroded after 2 days seawater incubation and the green patina was formed on the copper rods surface. Besides, the seawater colour was changed to blue-green colour after 3 days incubation. Formation of blue-green colour is caused by the corrosion of copper rod where finely divided insoluble flocculent of copper corrosion was suspended in water. The type of corrosion products depend on the actual water composition, but most likely were copper hydroxides with some silicate and sulphates.

The copper concentration in the seawater was measured using atomic absorption spectrometry. For the incubation period ranging from 1 to 7 days, the copper concentrations in the seawater were increased (Figures 4.1 and 4.2). Incubation of the bare copper rod (copper A) in the seawater resulted the highest copper concentration in the seawater. However, copper rods that coated with enamel coating (copper E) have the lowest copper concentration in the seawater. Besides, copper concentrations in the seawater with temperature of 25°C were relatively high if compared with seawater with temperature of 60°C.

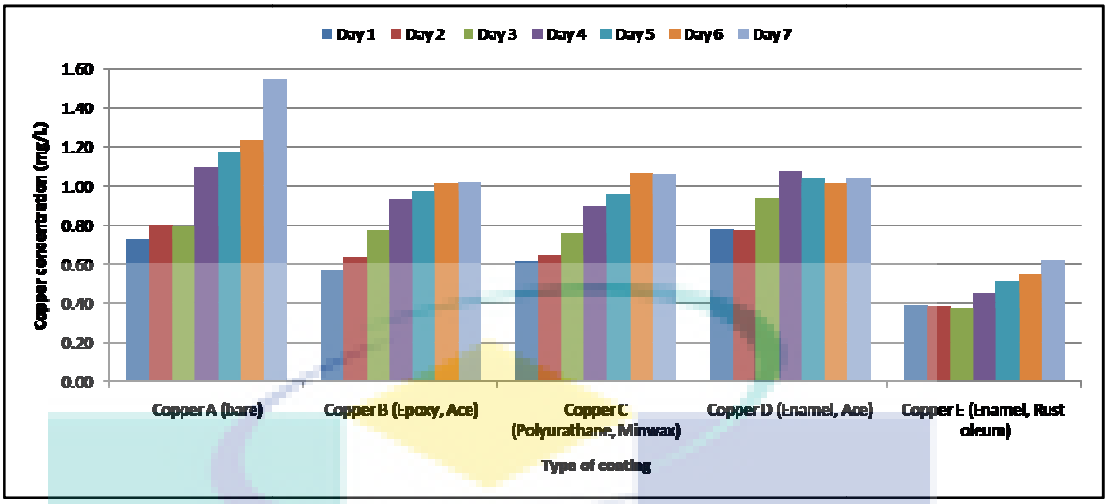

Figure 4.1: Effect of coating material and incubation period on copper concentration in seawater at 25°C incubation temperature.

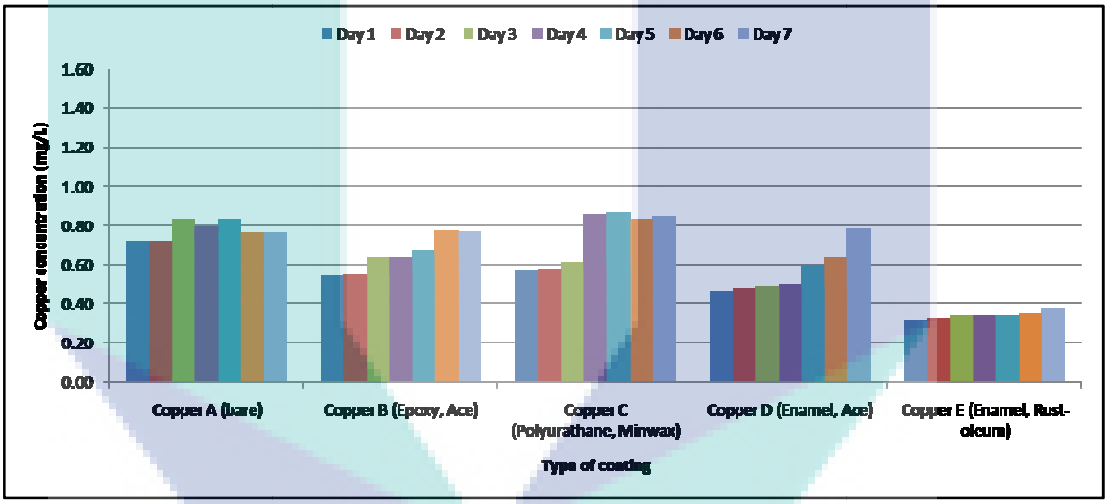

Figure 4.2: Effect of coating material and incubation period on copper concentration in seawater at 60°C incubation temperature.

By using the formula stated in Chapter 3, the copper rods weight loss and corrosion rate were calculated. The effects of coating material and incubation temperature on the weight loss and corrosion rate were studied and the results were tabulated in Figures 4.3 and 4.4, respectively. The findings confirm the previous results in which the bare copper rods (copper A) have the highest weight loss and corrosion rate if compared with copper rods coated with different coating material. Besides, weight loss and corrosion rate with incubation temperature of 25°C were also relatively high if compared with incubation temperature of 60°C.

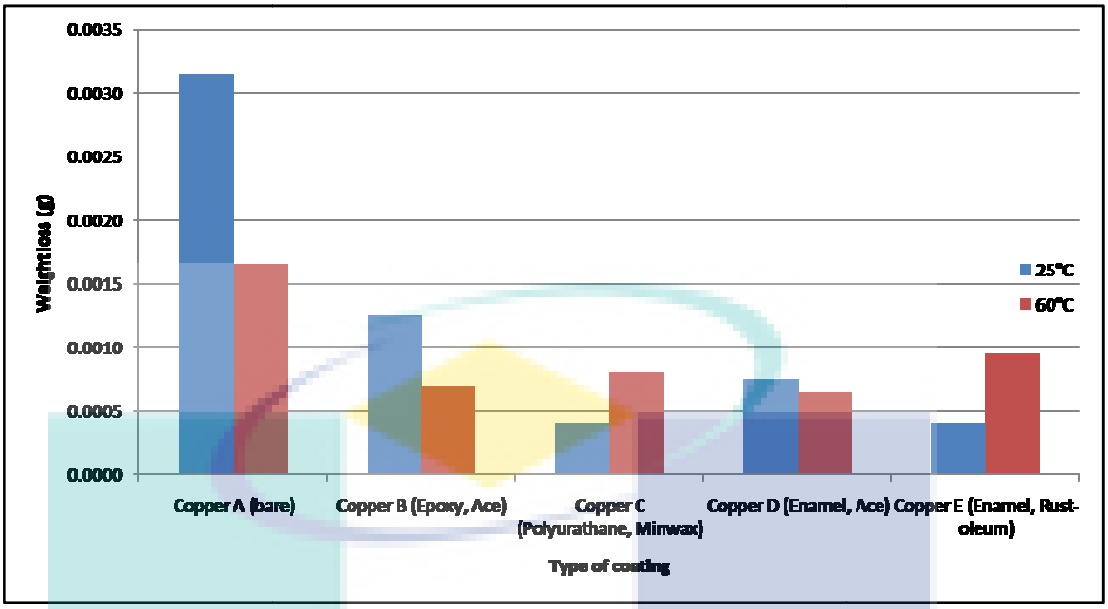

Figure 4.3: Effect of coating material and incubation temperature on weight loss of copper rod.

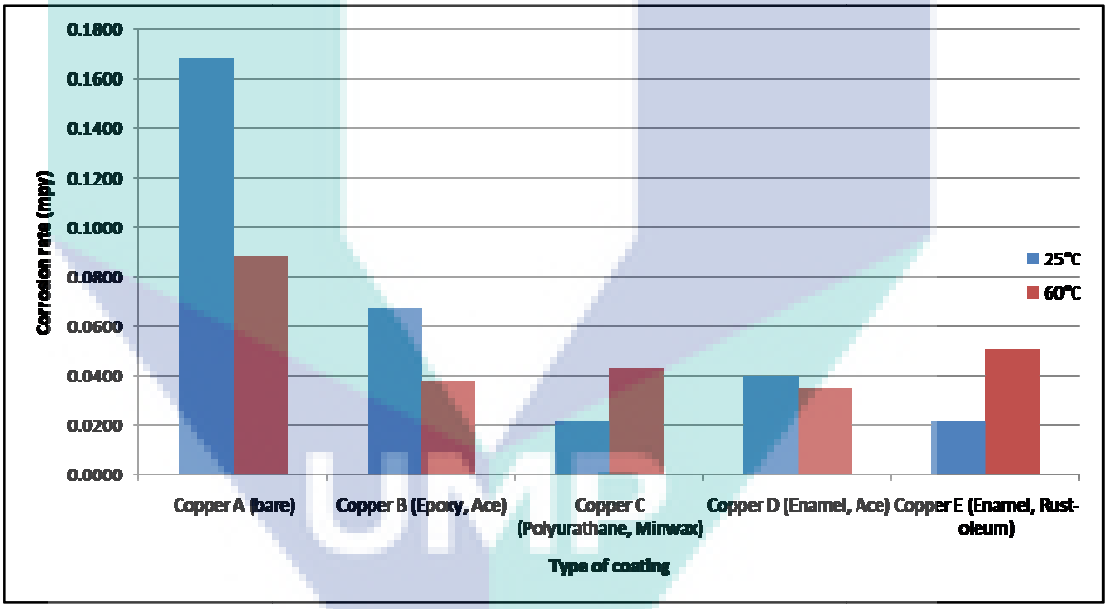

Figure 4.4: Effect of coating material and incubation temperature on corrosion rate.

Copper rods coated with different coating material have low corrosion rate if compared with bare copper rod. This is due to the paint coating that protects the copper rod from corrosion. It has been demonstrated in the literature in which the corrosion of copper can be prevented by using paint as the coating material. However, the copper concentration in the seawater increased when the incubation period of copper rods with coating (copper B to E) were increased. It was observed that the paint coatings start to break after few days of incubation. It can be classified as

uniform corrosion. When the paint coating was broken, intergranular corrosion can be examined and dispersed in the base copper. The intergranular corrosion might because of the thermal stress at elevated temperature. As demonstrated in this study, copper rods corrode at different rate at different temperature. The corrosion rates of copper rods at incubation temperature of 60°C were lower than the copper rods that incubated at temperature of 25°C. It has been demonstrated in the literature in which highest corrosion rate occurred between temperatures of 18 to 28°C.

4.2 Effect of coating material and thickness on heat transfer rate

Different coating layers were applied on the copper rods using various coating material for studying the effect of coating material and thickness on heat transfer rate. As expected, an increase in the coating layer increased the mass of the coated copper rods. By subtracting the mass of the coated copper rod from the bare copper rod, the mass of coating was determined (Figure 4.5). By using different coating material, the data in Figure 4.5 indicates that the number of coating layer was found to have a linear relationship with the coating mass ($R^2 > 0.95$). The way to apply the layers of coating material depended on the spraying skill in which spraying direction, angle and speed may affected the distribution of coating material on the copper rod. Spraying the coating material in shorter distance only covered less rod surface, however more paint was coated on the rod surface.

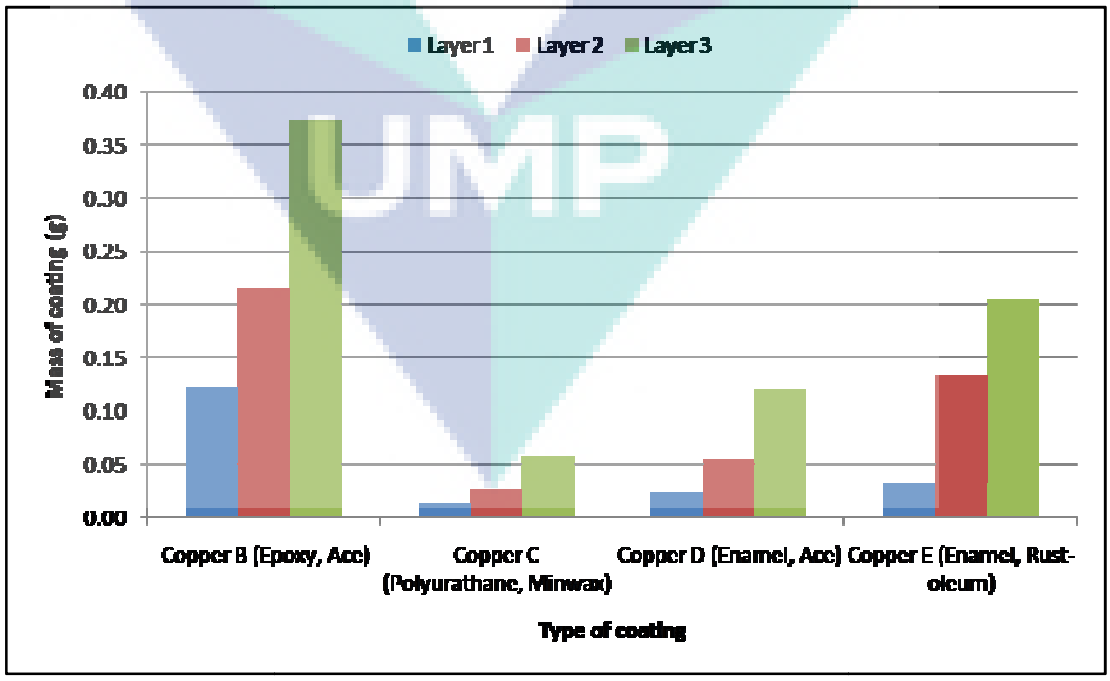

Figure 4.5: The mass of coating materials at different coating layers.

As shown in Figure 4.5, copper rods that coated with epoxy coating (copper B) has the highest coating mass. The detail chemical composition of different coating material is listed in Table 4.1. Epoxy coating consists high weight percent of titanium dioxide, which resulted the highest coating mass among the others coating materials. Besides, it is worthy to note that copper D and E were coated same coating material (enamel) but with different brand. The data in Figure 4.5 shows that coating mass of enamel coating with brand of Rust-oleum is higher than the enamel coating with brand of Ace. This can be explained by the chemical composition in these different types of enamel coatings, where enamel coating with brand of Rust-oleum has more chemical weight percent than the enamel coating with brand of Ace (Table 4.1). Copper rods that coated with polyurethane coating (copper C) has the lowest coating mass. This might due to the colourless paint which lack of the chemical additives such as titanium dioxide and colouring additive.

Table 4.1: The chemical composition of coating material.

Chemicals [weight (%)]	**Copper B (Epoxy, Ace)**	**Copper C (Polyurathane, Minwax)**	**Copper D (Enamel, Ace)**	**Copper E (Enamel, Rust-oleum)**
Acetone	23	-	33	25
Toluene	18	-	21	-
Propane	13.8	-	13.8	10
n-Butyl Acetate	12.2	-	-	10
n-Butane	13.2	-	13.2	2.5
Barium Sulfate	-	-	-	2.5
Solvent Naphtha, Light Aromatic	-	-	-	2.5
1,2,4-Trimethylbenzene	-	-	-	1.0
Propylene Glycol Monobutyl Ether	-	-	-	1.0
Titanium Dioxide	7.4	-	1.1	1.0
Ethyl benzene	-	-	-	0.1
Med. Aliphatic Hydrocarbon Solvent	-	3.0	-	-
Mineral Spirits	-	46.0	-	-
Amorphous Precipitated Silica	-	2.0	-	-

For axial heat transfer analysis, thermal conductivity of copper rods that coated with different coating materials and layers were determined (Figure 4.6). Under the steady-state condition, the thermal conductivities of copper B, D and E increased when the coating layer was increased further. It is worthy to note that these copper rod coating materials may improve the thermal conductivities which are higher than the thermal conductivity of the bare copper rod (388 W/m.K). In addition, the thermal conductivity of copper C decreased when second coating layer was applied. However, a further increase in the coating layer resulted in an increase of thermal conductivity.

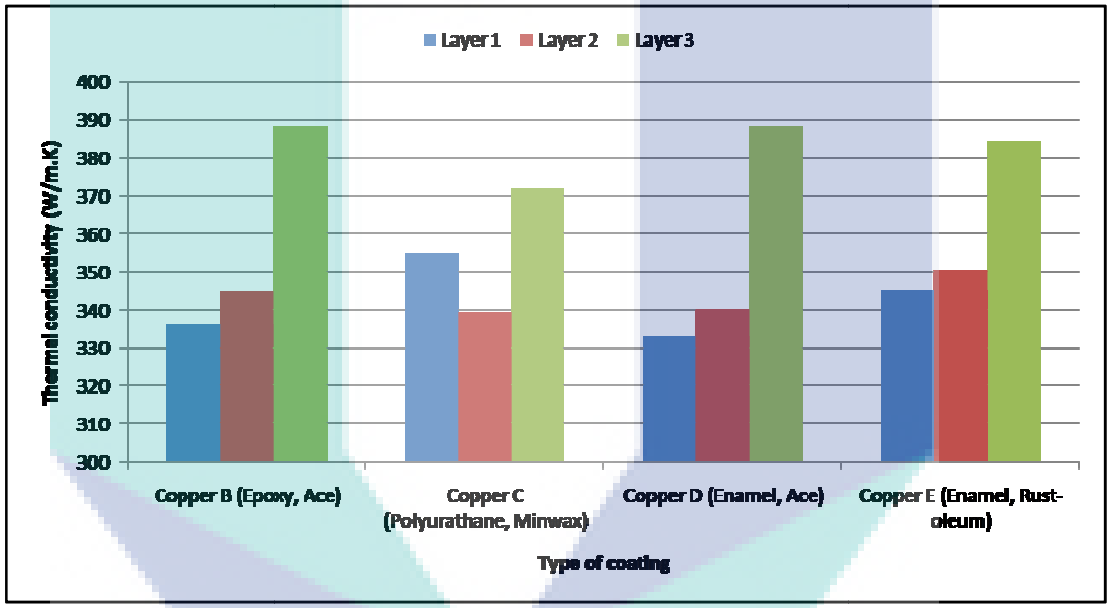

Figure 4.6: The thermal conductivity of coating materials at different coating layers.

Number the coating layer on the copper rods may affect the radial heat transfer rate, as well as the axial heat transfer rate. As demonstrated in this study, adding the coating layer reduced the radial heat transfer rate. Hence, thermal conductivities of copper B, D and E were increased and higher axial heat transfer rates were obtained. Moreover, the critical thickness of coating layer that causes the maximum radial heat transfer rate was investigated. If the coating layer thickness is lesser than the critical thickness, by adding more coating layers will increase the radial heat transfer rate, and hence decrease the axial heat transfer rate, and vice versa. As shown in Figure 4.7, copper B, D and E exhibit critical thickness between the first and second coating layer. Meanwhile, the critical thickness of copper C was at the second coating layer.

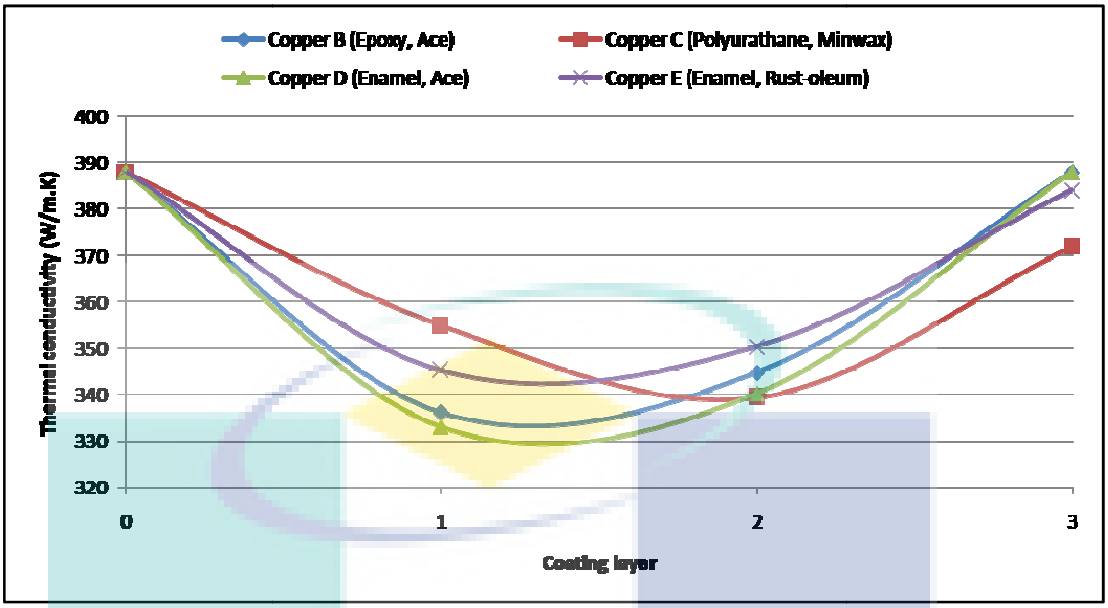

Figure 4.7: Critical thickness for heat transfer analysis.

4.3 Solar still fabrication with heat transfer agent

A solar still was fabricated in the shape of double slope single basin which allows the solar still to receive solar rays from both east and west direction in Malaysia. The solar still was built of wood and covered by aluminium framed glass at 45° angle with the horizontal line. Aspirator pump was installed to reduce the pressure inside the solar basin (Figure 4.8), hence water in the inner basin can be vaporised at a lower temperature. Besides, the aspirator pump was powered by a motor that able to pull out the vaporised water from the inner basin to the aspirator basin for condensation. To focus the amount of heat received, nine magnifying lenses were added to the solar still (Figure 4.9). In addition, measuring tools consist of a pyranometer to measure solar radiation, thermocouple sensors to measure temperature, and a vacuum pressure gauge to measure pressure, were installed on the solar still (Figure 4.10 a-c).

Figure 4.8: The aspirator pump.

Figure 4.9: The arrangement of magnifying lenses.

(a) (b) (c)

Figure 4.10: Measuring tools for solar still. (a) pyranometer; (b) thermocouple sensors; (c) vacuum pressure gauge.

Moreover, the height of the solar still was relatively higher than the existing solar still in the literature in order to install the HTA. HTA consists of a sheet of copper plate which acts as a receiving panel and 12 pieces of copper rods that attach under the copper plate (Figure 4.11). The thickness of the copper plate was designed with relevant thick in order to avoid bending when exposed under high solar energy. In the meantime, the copper plate also cannot be too thick that resulted high resistant for heat transfer to water. The rods were designed with relevant length that able to immerse in the water and distribute the heat. Copper metal has high thermal conductivity in which the collected solar energy may be transferred via conduction to the water. Copper and its alloys have been widely used in marine industry (Cato and Brown, 2003). The ability to resist corrosion is impressive compared to other metals.

Figure 4.11: The fabricated HTA.

The purpose of this research project is to develop a solar still has the ability to increase the water evaporation rate. The design of solar still unit that installed with aspirator pump, magnification lenses and HTA is shown in Figure 4.12. As demonstrated in this study, the present of the HTA in the solar still has improved the heat transfer rate and increase the water evaporation rate.

Figure 4.12: The designed solar still.

4.4 Solar still experiment analyses

The effect of HTA in the solar still was investigated. The experiment was started at 8 am until 5 pm and experimental data were collected in every hour for heat transfer study. Figures 4.13 and 4.14 show the temperature profile of the solar still without HTA and with HTA, respectively. The water temperature, T_w, glass temperature, T_g, and ambient temperature,T_a data were recorded in every hour from three chosen days (clear and cloudless day). As demonstrated in this study, the water and glass temperatures were higher than the ambient temperature. The temperatures increased

in the first five hours due to the available of solar radiation in the morning to the afternoon. The temperatures decreased after 12 noon. The water temperature and the glass temperature are varied several degrees centigrade as reported by Dev and Tiwari, 2009). Water and glass temperatures in vacuum solar still are between 40°C to 50°C, which are slightly lower than non-vacuum solar still (Al-Hussaini and Smith, 1995; Scott et al., 2005).

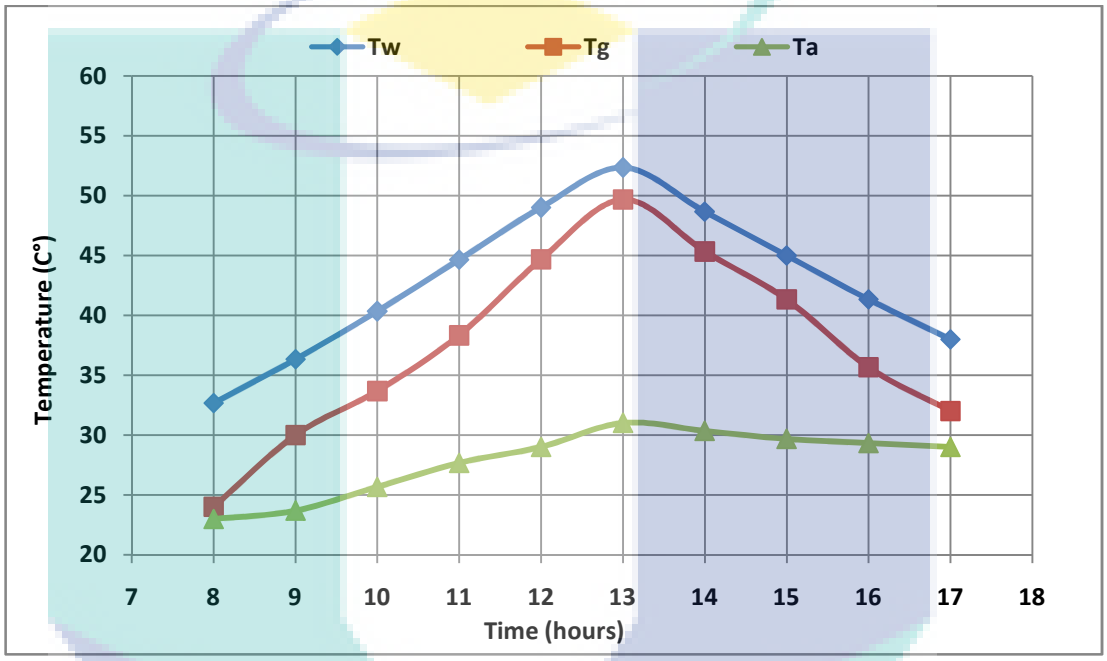

Figure 4.13: Temperature profile of solar still without HTA.

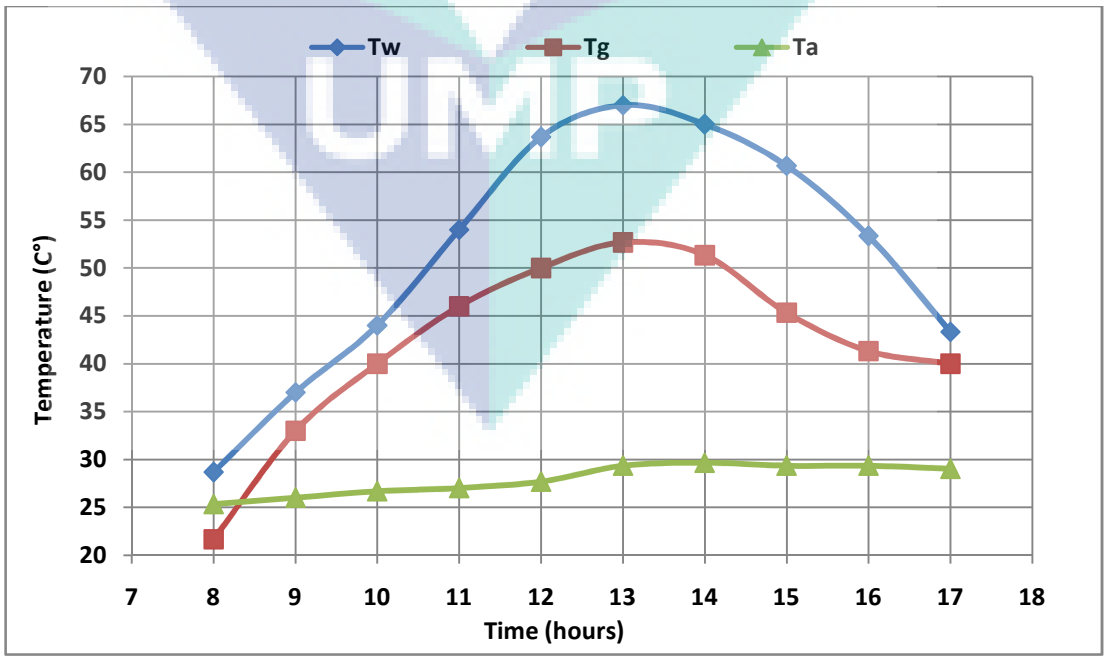

Figure 4.14: Temperature profile of solar still with HTA.

Comparison of water and glass temperatures for solar still with and without HTA was further investigated (Figures 4.15 and 4.16). In general, water and glass temperatures of solar still with HTA were higher than the solar still without HTA. This further confirmed the efficiency of the copper plate and rods as the HTA for heat transfer process.

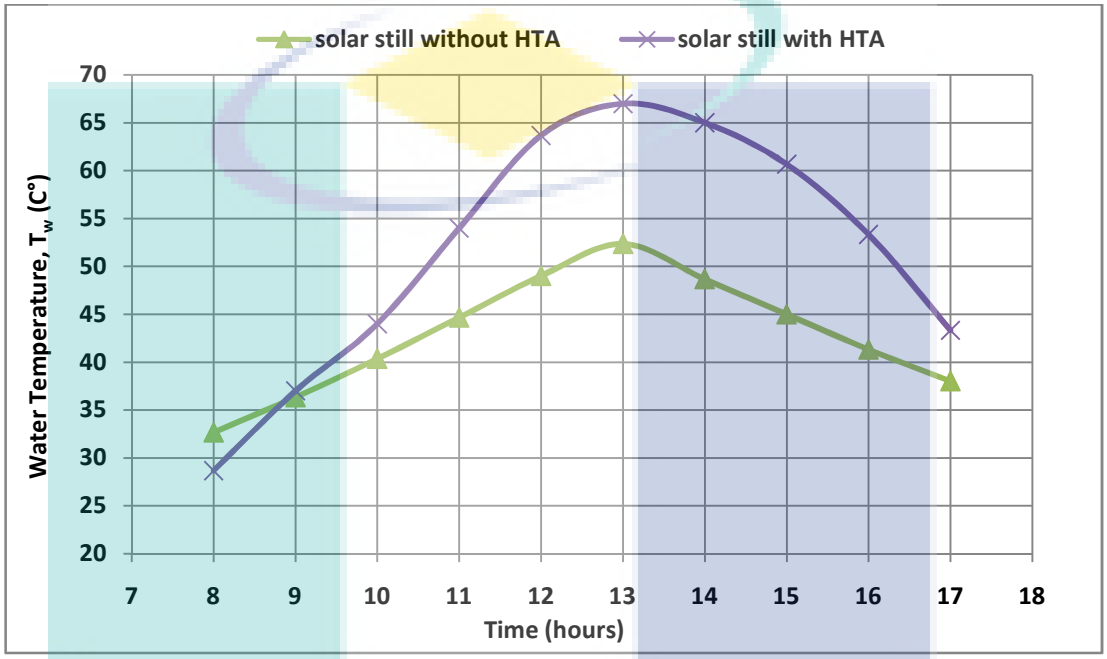

Figure 4.15: Comparison of water temperature for solar still with and without HTA.

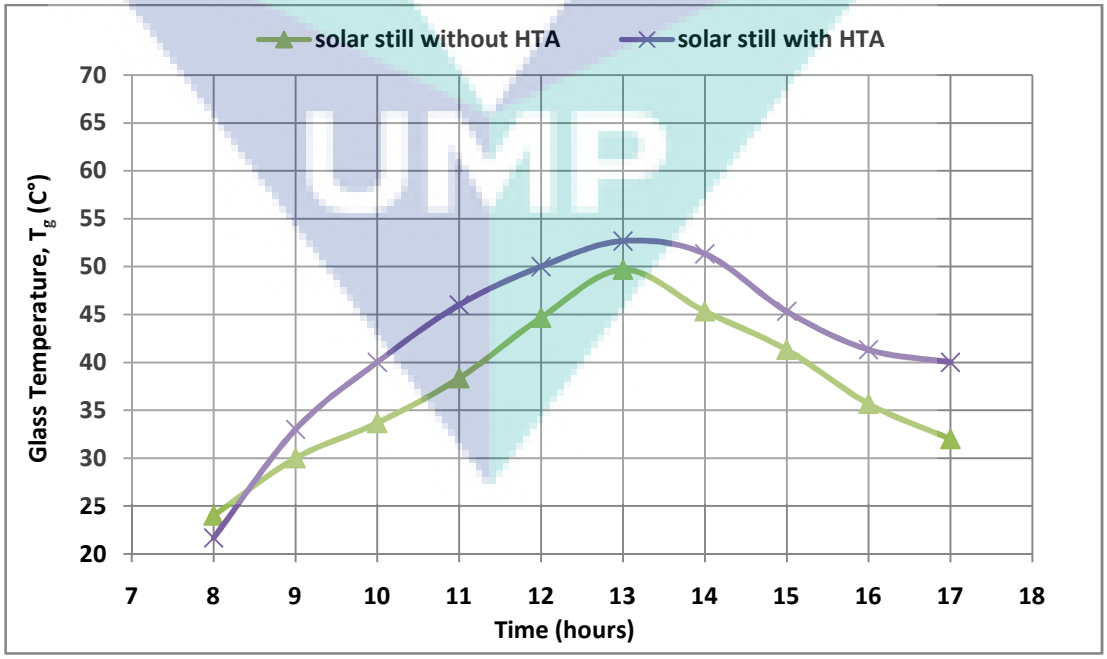

Figure 4.16: Comparison of glass temperature for solar still with and without HTA.

Besides, it is worthy to note that the available of the magnifying lenses affected the efficiency of the HTA. Water temperature of solar still with HTA but without magnifying lenses were lower than the solar still with HTA and magnifying lens (data not shown). Without the magnifying lenses, the existing of HTA has created a thermal resistance for the solar rays from reaching the water surface and leading to the low water temperature. However, the present of magnification lenses may focus the radiation energy from the sunrays on the HTA. During the 10 hours of experiment, HTA always exhibit higher temperature if compare with water temperature (Figure 4.17) Thus, it reveals the function of the copper plate and rods that may transferred the radiation energy from the HTA to the water.

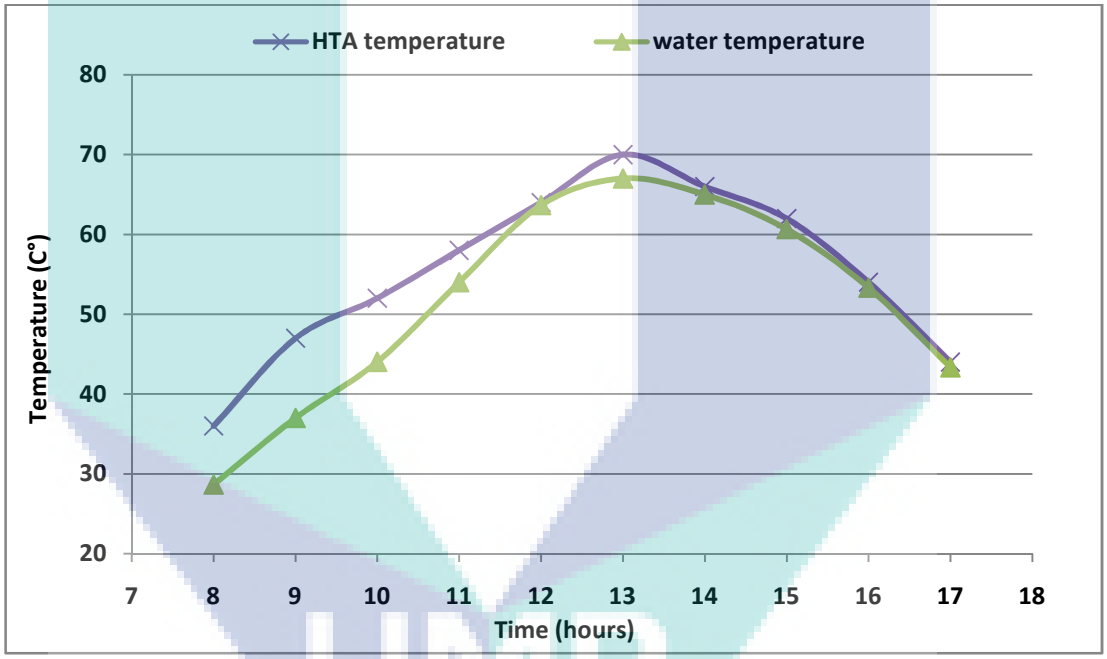

Figure 4.17: HTA and water temperature for solar still with HTA.

The intensity of the solar radiation that received by solar still is one of the important parameter that affects the water evaporation rate of the solar still (Ahsan et al., 2013; Nafey et al., 2000). Figures 4.18 and 4.19 show the solar radiation and evaporation rate of the solar still without HTA and with HTA, respectively. The solar radiation and water evaporation rate increased in the first six hours due to the available of solar radiation in the morning to the afternoon. The solar radiation and water evaporation rate of the solar still decreased after 1 pm. The maximum water evaporation rate occurred between 1-3 pm in which high water temperature and solar radiation were obtained. After 1 pm, the reduction of water evaporation rate was not critical. This

might due to the solar still that acted as a greenhouse in which the trapped radiation energy keeps evaporating the water after solar radiation was faded.

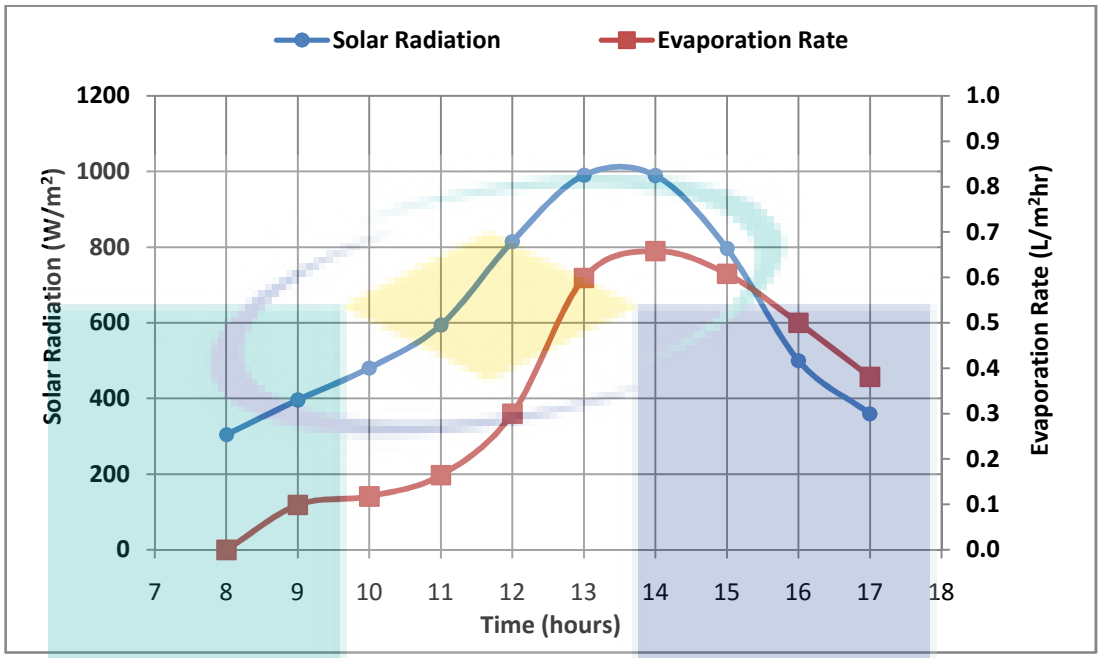

Figure 4.18: Solar radiation and evaporation rate of solar still without HTA.

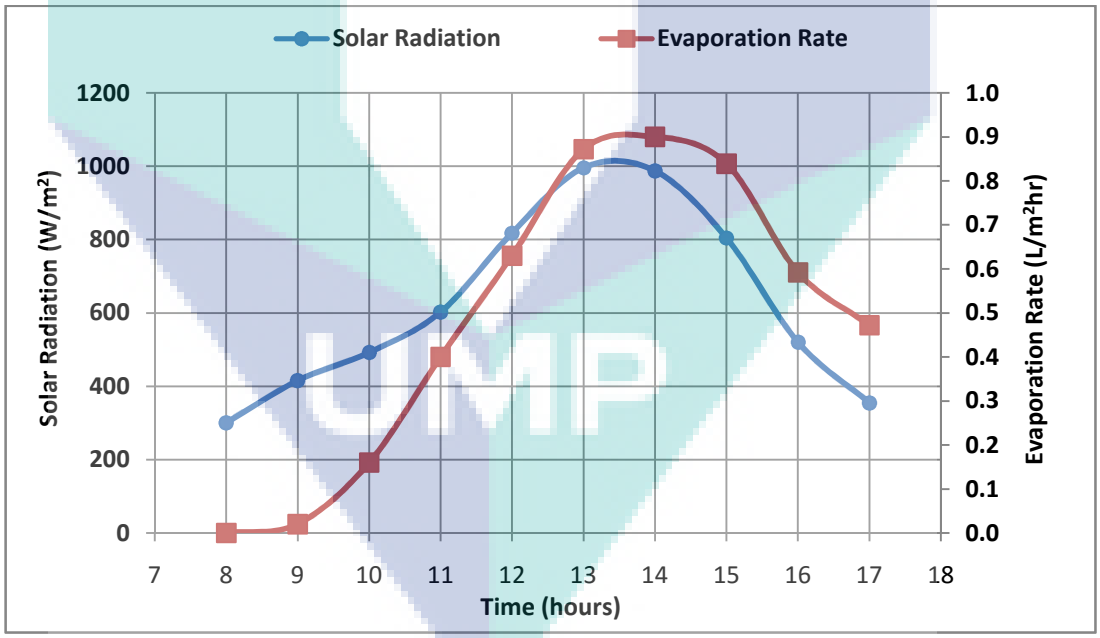

Figure 4.19: Solar radiation and evaporation rate of solar still with HTA.

Comparison of solar radiation and evaporation rate for solar still with and without HTA was further investigated (Figures 4.16 and 4.17). During the experiment, no variation on solar radiation was discovered for solar still with and without HTA. This result confirms the earlier report in which average daily solar radiation in Kuantan,

Pahang is about 4.57 kW/m^2 (Engel-Cox et al., 2012). In general, evaporation rate of solar still with HTA were higher than the solar still without HTA. The presence of the copper plate and rods as the HTA has promptly heated the liquid water closed to the vapour phase. Hence, the water molecules that held higher energy could vaporised easily.

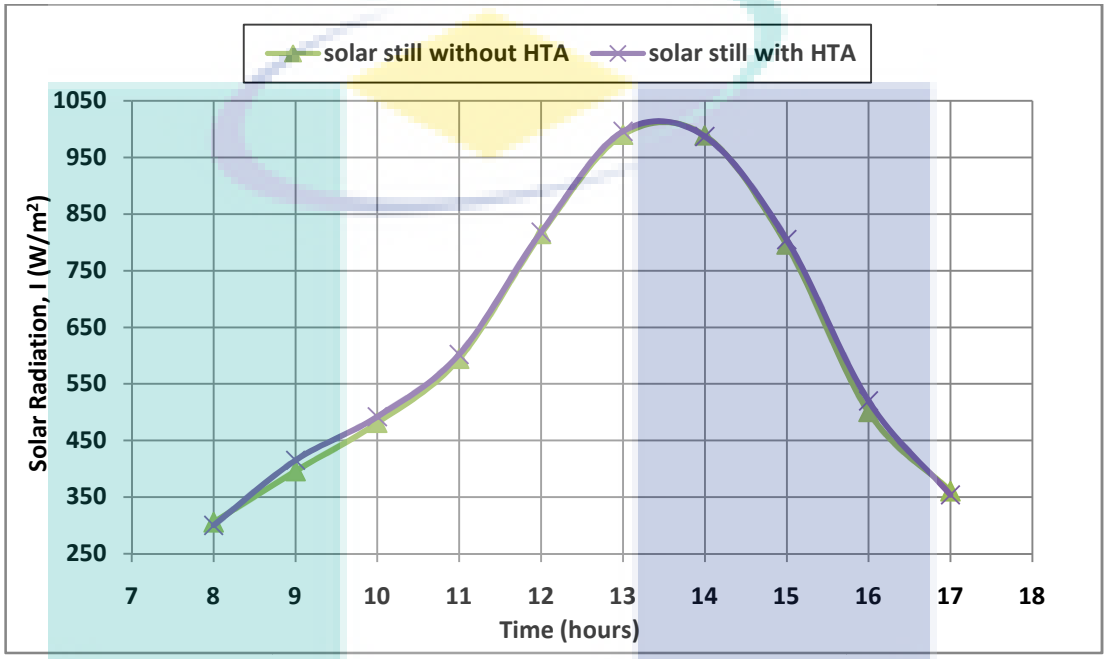

Figure 4.20: Comparison of solar radiation for solar still with and without HTA.

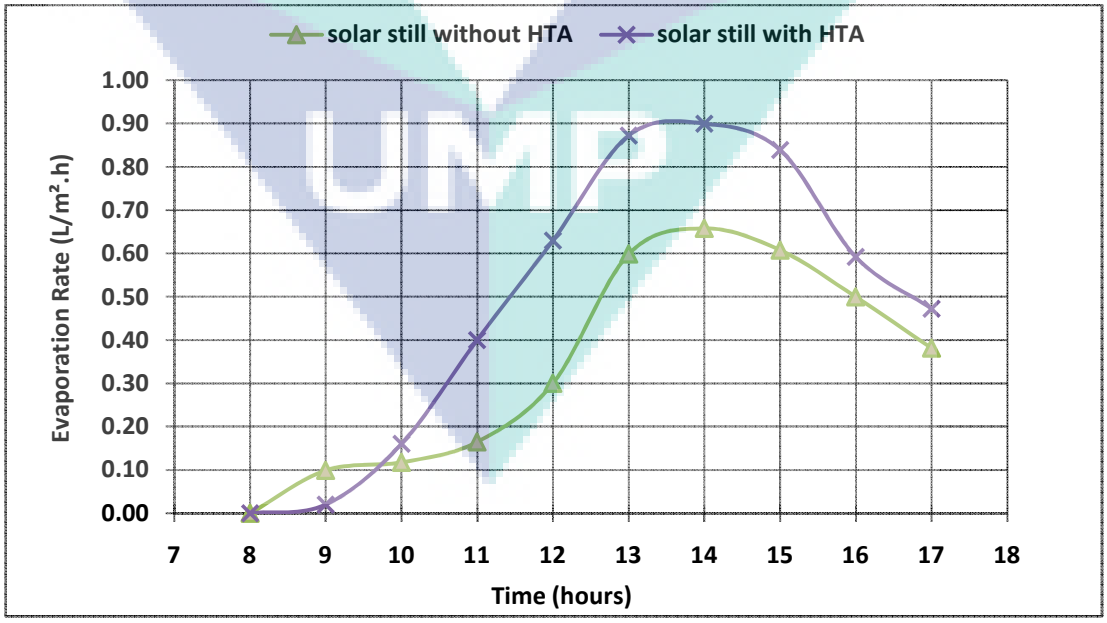

Figure 4.21: Comparison of evaporation rate for solar still with and without HTA.

In addition, total water evaporation rate was calculated for the nine hours experiment. Under the same solar radiation, the total evaporation rate of solar still with HTA was 4.89 L/m^2.h which was 30% higher than the solar still without HTA. These situations agreed by the earlier researchers in which more water vaporised if greater the amount of the energy was received (Sampathkumar et al., 2010; Omara et al., 2013; Pillai et al., 2015). Solar still with magnifying lenses and HTA may receive high amount of radiation energy and the energy was transferred quickly through copper plate and rods into the water. This can be further confirmed the efficiency of the HTA in improving the water evaporation rate of solar still.

The heat transfer occurs inside the solar still system using radiation, convection, and evaporation mechanisms. In this study, aspirator was installed with the solar still in which vacuum condition was applied. No the heat transfer by convection has occurred because no diffusion of vapour through the air that acted as medium for convective heat transfer. Therefore, the major mechanisms of heat transfer that takes place inside the vacuum solar still is radiative heat transfer and evaporation. For solar still heat transfer analysis using energy balance equation and technical specification in Table 4.2, the evaporative heat transfer (q_{ewg}) that occurred from water to glass of solar still without HTA was determined and the evaporative heat transfer (q_{eHg}) that occurred from HTA to glass of solar still with HTA was calculated (Figure 4.22).

Table 4.2: Technical specification for evaporative heat transfer determination.

Specifications / Parameters	Dimensions / Values
Basin area, A_b	0.3 m^2
HTA area, A_H	0.2 m^2
Thermal conductivity of HTA, K	395 W/m.K(Perry and Green, 1984)
Glass transmissivity, τ_g	0.9 (Siegenthaler, 2014)
Heat capacity of water , C_w	0.7615 x10^5 J/kmol.K(Perry and Green, 1984)
Glass emissivity, ε_g	0.937 (Perry and Green, 1984)
HTA absorptivity, α_H	0.9 (Bolz, 1973)
Stefan Boltzmann constant, σ	5.67 x 10^{-8} W/m^2.K^4(Perry and Green, 1984)

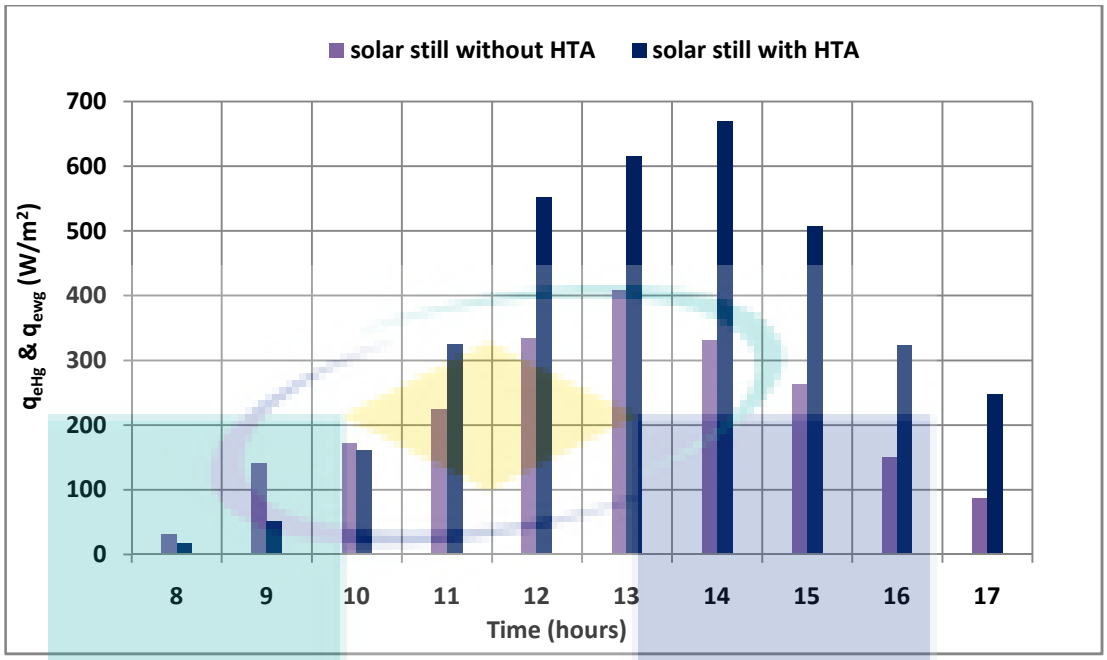

Figure 4.22: Evaporative heat transfer for solar still with and without HTA.

Figure 4.22 demonstrated that the evaporative heat transfer rate of solar still increased in the first six and seven hours due to the available of solar radiation in the morning to the afternoon and decreased after 1 to 2 pm. Again, evaporative heat transfer of solar still with HTA were higher than the solar still without HTA. Besides, thermal efficiency that defined as the ratio between the energy that has been consumed to contributed for the heat capacity of the water mass inside the basin to the global solar radiation energy received by the solar still (Garg, 2000) was determined. Experiment result revealed that the introduction of HTA into the solar still has successfully increase 18% of thermal efficiency (data not shown).

CHAPTER 5

CONCLUSIONS AND RECOMMENDATIONS

5.1 Conclusions

Seawater may cause copper rod corrosion. The copper concentrations in the seawater were increased when the bare and coated copper rods were immersed into the seawater for 7 days. Copper rods that coated with enamel coating (copper E) have the lowest copper concentration in the seawater. Besides, copper rods coated with different coating material have low weight loss and corrosion rate if compared with bare copper rod. This is due to the paint coating that protects the copper rod from corrosion. Besides, copper rods corrode at different rate at different temperature. Weight loss and corrosion rate with incubation temperature of 25°C were relatively high if compared with incubation temperature of 60°C.

An increase in the coating layer linearly increased the mass of the coated copper rods. Copper rods that coated with epoxy coating (copper B) has the highest coating mass, however, copper rods that coated with polyurethane coating (copper C) has the lowest coating mass. The mass of coating was depended on the chemical composition of different coating material. Under the steady-state condition, the thermal conductivities of copper B, D and E increased when the coating layer was increased further. Hence, adding the coating layer reduced the radial heat transfer rate and higher axial heat transfer rates were obtained. Besides, the thermal conductivity of copper C decreased when second coating layer was applied. However, a further increase in the coating layer resulted in an increase of thermal conductivity. As demonstrate in this study, copper B, D and E exhibit critical thickness between the first and second coating layer. Meanwhile, the critical thickness of copper C was at the second coating layer.

A solar still was designed and fabricated. HTA consists of a sheet of copper plate and 12 pieces of copper rods that attach under the copper plate. Two set of experiment set-up (solar still without HTA and solar still with HTA) were conducted under consistent solar radiation to investigate the effect of HTA on the solar still performance. In general, water and glass temperatures and evaporative heat transfer

of solar still with HTA were higher than the solar still without HTA. Experiment data have revealed the function of the HTA that may quickly transferred the radiation energy from the copper plate and rods to the water. The introduction of the HTA has successfully increased 30% of water evaporation rate and 18% of thermal efficiency.

5.2 Recommendations

There are some recommendations for further improve the research:

a. The composition of the copper rod should be determined for better understanding of corrosion rate and heat transfer rate.
b. An additional water basin for collecting condensed water vapour is recommended to installed, hence the solar still may properly measure the productivity.
c. The effect of water level on the evaporation rate may be investigated.
d. The performance of modified solar still can be practically tested for seawater.
e. All studied factors for the solar still can be further investigated and optimised using statistical optimisation software.

REFERENCES

ABDALLAH, S., ABU-KHADER, M. M. & BADRAN, O. 2009. Effect of various absorbing materials on the thermal performance of solar stills. *Desalination,* 242**,** 128-137.

ABDALLAH, S. & BADRAN, O. 2008. Sun tracking system for productivity enhancement of solar still. *Desalination,* 220**,** 669-676.

ADRIAENS, F. A. 2012. Influence of pH and chloride concentration on the corrosion behavior of unalloyed copper in NaCl solution: A comparative study between the micro and macro scales . *Materials* 5**,** 2439-2464.

AHSAN, A., RAHMAN, A., SHANABLEH, A., NIK DAUD, N., MOHAMMED, T. & MABROUK, A. 2013. Life cycle cost analysis of a sustainable solar water distillation technique. *Desalination and Water Treatment,* 51**,** 7412-7419.

AL-HUSSAINI, H. & SMITH, I. 1995. Enhancing of solar still productivity using vacuum technology. *Energy conversion and management,* 36**,** 1047-1051.

BADRAN, A. A., ASSAF, L. M., KAYED, K. S., GHAITH, F. A. & HAMMASH, M. I. 2004. Simulation and experimental study for an inverted trickle solar still. *Desalination,* 164**,** 77-85.

BADRAN, O. 2007. Experimental study of the enhancement parameters on a single slope solar still productivity. *Desalination,* 209**,** 136-143.

BADRAN, O., BEITHOU, N., ALAWIN, A. A., AWAD, A., ABDELHADI, Y. & AL-MOFLEH, A. 2013. Experimental Study of a Vacuumed Solar Still System. *International Journal of Applied Power Engineering (IJAPE)* 2**,** 99-104.

BHATTACHARYYA, A. 2013. Solar stills for desalination of water in rural households. *International Journal of Environment and Sustainability*.

BOLZ, R. E. 1973. *CRC handbook of tables for applied engineering science*, CRC press.

BOZKURT, I., ATIZ, A., KARAKILCIK, M. & DINCER, I. 2014. An investigation of the effect of transparent covers on the performance of cylindrical solar ponds. *International Journal of Green Energy,* 11**,** 404-416.

CIPOLLINA, A., MICALE, G. & RIZZUTI, L. 2009. Seawater desalination: conventional and renewable energy processes. *Springer Science & Business Media.*

CATO, J. C. & BROWN, C. L. 2003. Marine Ornamental Species: Collection, Culture and Conservation, *Iowa State, Iowa State Press.*

CHANDLER, K. A. 1985. Paint coatings. *In Marine and Offshore Corrosion* 204-232.

CHARLES C P. Jr, C. 1948. Experimental determination of the thermal conductivity of porous copper.

DAVIS, J. R. 2001. *Copper and Copper Alloys*, ASM International.

DEV, R. & TIWARI, G. 2009. Characteristic equation of a passive solar still. *Desalination*, 245**,** 246-265.

DEXTER, S. C. 1995. Galvanic corrosion. *Mas Note From the University of Delaware Sea Grant Marine Advisory Service*, 645.

ELDALIL, K. M. 2010. Improving the performance of solar still using vibratory harmonic effect. *Desalination*, 251**,** 3-11.

EL-SEBAII, A., ABOUL-ENEIN, S. & EL-BIALY, E. 2000a. Single basin solar still with baffle suspended absorber. *Energy conversion and management*, 41**,** 661-675.

EL-SEBAII, A., ABOUL-ENEIN, S., RAMADAN, M. & EL-BIALY, E. 2000b. Year-round performance of a modified single-basin solar still with mica plate as a suspended absorber. *Energy*, 25**,** 35-49.

ENGEL-COX, J., NAIR, N. & FORD, J. 2012. Evaluation of solar and meteorological data relevant to solar energy technology performance in Malaysia. *Journal of Sustainable Energy & Environment*, 3**,** 115-124.

FENG, Y. 1997. Corrosion mechanisms and products of copper in aqueous solutions at various pH values. *Corrosion Science* 389-398.

GARG, H. 2000. Solar energy: fundamentals and applications, *Tata McGraw-Hill Education.*

GNANADASON, M. K., HARIHARAN, G. & KUMAR, P. S. 2013. Enhanced Performance of Design of a Single Basin Solar Still made up of Copper. *Indian Journal of Applied Research*, 3**,** 299-302.

GNANADASON, M. K., KUMAR, P. S., SIVARAMAN, G. & DANIEL, J. E. S. 2011. Design and performance analysis of a modified vacuum single basin solar still. *Smart Grid and Renewable Energy*, 2**,** 388.

GNANADASON, M. K., KUMAR, P. S., WILSON, V. H. & KUMARAVEL, A. 2015. Productivity enhancement of a-single basin solar still. *Desalination and Water Treatment*, 55**,** 1998-2008.

KHALIFA, A. J. N. 2011. On the effect of cover tilt angle of the simple solar still on its productivity in different seasons and latitudes. *Energy conversion and management*, 52**,** 431-436.

KINGSLEY, O. & OPARAODU, G. C. 2014. Comparison of percentage weight loss and corrosion rate trends in different metal coupons from two soil environments. *International Journal of Environmental Bioremediation & Biodegradation,* 5**,** 243-249.

KUMAR, B. S., KUMAR, S. & JAYAPRAKASH, R. 2008. Performance analysis of a "V" type solar still using a charcoal absorber and a boosting mirror. *Desalination,* 229**,** 217-230.

LU, L. 2005. Experimental study of crevice corrosion of copper. *Canada: University of Saskatchewan.*

MARS G. & FONTANA, L. M. 2005. The eight forms of corrosion and the corrective measures. 137-148.

MELCHERS, R. E. 2001. Temperature effect on seawater immersion corrosion of 90:10 copper-nickel alloy. *Corrosion Science* 57**,** 440-451.

MURUGAVEL, K. K., CHOCKALINGAM, K. K. & SRITHAR, K. 2008. Progresses in improving the effectiveness of the single basin passive solar still. *Desalination,* 220**,** 677-686.

NAFEY, A. S., ABDELKADER, M., ABDELMOTALIP, A. & MABROUK, A. 2000. Parameters affecting solar still productivity. *Energy Conversion and Management,* 41**,** 1797-1809.

NAFEY, A. S., ABDELKADER, M., ABDELMOTALIP, A. & MABROUK, A. 2002. Enhancement of solar still productivity using floating perforated black plate. *Energy Conversion and Management,* 43**,** 937-946.

NITHIN, P. K. & HRAIHARAN, R. 2014. Experimental Analysis of Double Effect Type Solar Still Integrated with Liquid Flat Plate Collector. *International Journal of Emerging Engineering Research and Technology* 2**,** 240-247.

OMARA, Z., ELTAWIL, M. A. & ELNASHAR, E. A. 2013. A new hybrid desalination system using wicks/solar still and evacuated solar water heater. *Desalination,* 325**,** 56-64.

PAPPAS, S. 2014. Facts about copper. *Live Science*.

PATRICK A.C. & GANE, C. J. 2007. Heat transfer through calcium carbonate-based coating structures: Observation and model for a thermal fusing process. *Publication,* 1-52.

PERRY, R. H. & GREEN, D. W. 1984. Perry Chemical Engineering's Handbook. *Mc. Graw-Hill, Japan*.

PHILIP, A. & SCHWEITZER, P. K. 1996. Copper and Copper Alloys‖. In P. A. Schweitzer, *Corrosion Engineering Handbook, Second Edition - 3 Volume Set* (pp. 125-152). New York: Marcel Dekker, Inc.

PILLAI, R., LIBIN, A. & MANI, M. 2015. Study into solar-still performance under sealed and unsealed conditions. *International Journal of Low-Carbon Technologies,* 10**,** 354-364.

RABADIA, C. 2015. Factors Influencing the Productivity of Solar Still.

SALEH A. & AL-FOZAN, A. U. 2008. Effect of seawater level on corrosion behavior of different alloys. *Desalination* 228**,** 61-67.

SAMEE, M. A., MIRZA, U. K., MAJEED, T. & AHMAD, N. 2007. Design and performance of a simple single basin solar still. *Renewable and Sustainable Energy Reviews,* 11**,** 543-549.

SAMPATHKUMAR, K., ARJUNAN, T., PITCHANDI, P. & SENTHILKUMAR, P. 2010. Active solar distillation - A detailed review. *Renewable and Sustainable Energy Reviews,* 14**,** 1503-1526.

SCOTT, L., SIVAKUMAR, M. & HAGARE, D. 2005. Perspectives on solar distillation: A review.

SHANMUGAN, S., JANARTHANAN, B. & CHANDRASEKARAN, J. 2012. Performance of single-slope single-basin solar still with sensible heat storage materials. *Desalination and Water Treatment,* 41**,** 195-203.

SIEGENTHALER, J. 2014. Heating with renewable energy.

SINGHA, N. 2013. Performance analysis of single slope solar stills at different inclination angles: An indoor simulation.

SUDHIR ACHAR, L. J. 2013. Developments in waterborne thermal insulation coating. *JPCL*.

TABRIZI, F. F. & SHARAK, A. Z. 2010. Experimental study of an integrated basin solar still with a sandy heat reservoir. *Desalination,* 253**,** 195-199.

TANAKA, H. & NAKATAKE, Y. 2005. A simple and highly productive solar still: a vertical multiple-effect diffusion-type solar still coupled with a flat-plate mirror. *Desalination,* 173**,** 287-300.

TIWARI, A. K. & TIWARI, G. 2006. Effect of water depths on heat and mass transfer in a passive solar still: in summer climatic condition. *Desalination,* 195**,** 78-94.

VALSARAJ, P. 2002. An experimental study on solar distillation in a single slope basin still by surface heating the water mass. *Renewable Energy,* 25**,** 607-612.

VELMURUGAN, V., GOPALAKRISHNAN, M., RAGHU, R. & SRITHAR, K. 2008. Single basin solar still with fin for enhancing productivity. *Energy Conversion and Management,* 49**,** 2602-2608.

WAN NIK, F. Z. 2011. Corrosion behavior of mild steel in seawater from two different sites of Kuala Terengganu coastal area. *International Journal of Basic & Applied Sciences* 11**,** 75-80.

ZEDAN, A. & ELDIN, S. N. 2015. An Experimental Investigation of the Factors Which Affect on the Performance of a Single Basin Typical Double Slope Solar Still for Water Desalination. *Energy and Power Engineering,* 7**,** 270.

ZURIGAT, Y. H. & ABU-ARABI, M. K. 2004. Modelling and performance analysis of a regenerative solar desalination unit. *Applied Thermal Engineering,* 24**,** 1061-1072.

APPENDIX

VOL. 11, NO. 10, MAY 2016 ISSN 1819-6608
ARPN Journal of Engineering and Applied Sciences

www.arpnjournals.com

SOLAR STILL: WATER FOR THE FUTURE

S. Nudra S. A. Aziz, Omar el Hadad, Syarifah A. Rahim and Chew F. Ne
Faculty of Chemical & Natural Resources Engineering, University Malaysia Pahang, Lebuhraya Tun Razak, Pahang, Malaysia
E-Mail: nudra_89@yahoo.com

ABSTRACT

Being an abundant natural resource that covers three quarters of the earth's surface, water still a major issue, as less than 1% of fresh water is actually within human reach. Solar energy, most recommended renewable energy source is widely used in desalination fields. Solar distillation, particularly solar still is expected to solve this fresh water production problem without causing any fossil energy depletion, hydrocarbon pollution and environmental degradation. However, the efficiency of the solar still is debatable. As the main reason of low productivity in a solar still is the low heat transfer inside the unit itself therefore, a thoroughly modification on solar still design is presented based on the scope of increasing the heat transfer process inside the unit. Significantly, introducing optical controlling techniques together with focused sunlight receiver and having the process to operate under low pressure have speed up the rate of production within 10 hours of day light. However, the presence of focused sunlight receiver is not seem to improve the production of the solar still yet an increase value is recorded.

MULTIMEDIA UNIVERSITY®

Certificate of Participation

This certificate is presented to

Dr. Chew Few Ne

In sincere appreciation for your participation in

"INTERNATIONAL ENGINEERING & TECHNOLOGY EXHIBITION 2015"

For university level, in category **Green Technology/Biotechnology**

On 24th - 25th Oct 2015 at Multimedia University, Melaka, Malaysia

Prof. Dr Ahmad Rafi bin Mohamed Eshaq
Vice President (Academic) of Multimedia University

TM Education Group

Universiti Malaysia PAHANG

FluidsChE 2015

CARIFF

CERTIFICATE OF RECOGNITION

This is to certify that

SITI NUDRA SHAFINIE BT AB AZIZ

has participated in The International Conference on Fluids & Chemical Engineering (FluidsChE 2015) organised by Center of Excellence for Advanced Research in Fluid Flow (CARIFF), Universiti Malaysia Pahang on 25-27 November 2015, at Adya Hotel Langkawi, Malaysia.

Assoc. Prof. Dr. Hayder A Abdulbari
FluidsChE 2015 Chair